A New Morphological Image Segmentation with Application in 3D Echographic Images

MIHAELA LASCU, DAN LASCU
Department of Measurements and Optical Electronics
Department of Applied Electronics
Faculty of Electronics and Telecommunications
Bd. Vasile Pârvan no.2
ROMANIA
mihaela.lascu@etc.utt.ro, dan.lascu@etc.utt.ro
http://www.etc.upt.ro

Abstract: This paper reviews ultrasound segmentation methods, in a broad sense, focusing on techniques developed for medical ultrasound images. Segmenting abnormal from normal myocardium using high-frequency intracardiac echocardiography (ICE) the 3D real-time images present new challenges for image processing in LabVIEW. Gray-level intensity and texture features of ICE images of myocardium with the same structural/perfusion properties differ. There are significant limitation conflicts with the existing segmentation techniques. The novelty of this paper consists of a new seeded region growing method to overcome the limitations of the existing segmentation techniques. The segmentation techniques are implemented using graphical programming LabVIEW and Vision. We use three criteria for region growing control: First, each voxel is merged into the globally closest region in the multifeature space. Second structural similarity is introduced to overcome the problem that myocardial tissue, despite having the same property, may be segmented into several different regions using existing segmentation methods. Third equal opportunity competence criterion is employed making results independent of processing order. This novel watershed segmentation method is applied to *in vivo* intracardiac ultrasound images using pathology as the reference method for the ground truth. The corresponding results demonstrate that this method is reliable and effective.

Key-Words: - ultrasound, echocardiography, graphical programming, watershed transform, watershed segmentation, image processing, LabVIEW, Vision.

1 Introduction

Three-dimensional echocardiography is a relatively new imaging modality and image analysis is not yet well developed. Early work used either freehand ultrasound with 2-D image acquisition synchronized with recording the location of the slice with a position sensor, rotational 3-D probes, which acquired a sparse set of 2-D image sequences, or real-time 3-D echocardiography based on the Volumetrics system [1], [2], [3].

However, a second generation of real-time 3-D echocardiography systems has recently been produced by Philips Medical Systems. This data is of higher quality than the rotational 3-D probe and Volumetrics systems [4]. One, therefore, has to take particular care in interpreting the results from early 3-D work as being representative of what it is possible to achieve today.

Ultrasound (US) image segmentation is strongly influenced by the quality of data. There are characteristic artefacts which make the segmentation task complicated, such as attenuation, speckle, shadows, and signal dropout; due to the orientation dependence of acquisition that can result in missing boundaries. Further complications arise as the contrast between areas of interest is often low. The scientific novelty of this paper consists of a new seeded region growing method to overcome the limitations of the existing segmentation techniques.

However, there have been recent advances in transducer design, spatial/temporal resolution, digital systems, portability, etc., that mean that the quality of information from an ultrasound device has significantly improved. This has led to increased use of ultrasound in not only its traditional area of application, diagnosis and CAD, but also emerging areas such as image-guided interventions and therapy. Thus, there is currently a re-emergence of interest in understanding how to do one of the oldest image processing tasks, image segmentation, applied to ultrasound data. As this paper attempts to demonstrate, while in other areas of medical imaging, notably X-ray computed tomography (CT) and magnetic resonance imaging (MRI), application

of general image processing methods can suffice, in the case of ultrasound data, customized methods, which attempt to model the imaging physics in some way have proven to be more successful. This paper focuses on techniques developed for native conventional *B* - mode ultrasound images and not segmentation of radio-frequency (RF) signal or Doppler images. Both two-dimensional (2-D) and three-dimensional (3-D) segmentation are considered, although the literature on 2-D methodology is far more extensive, reflecting the still relatively low , but increasing use of 3-D image acquisition technology in clinical practice today. B-Mode ultrasound imaging collects the same information, but adds a sense of direction, where the echo is coming from a two-dimensional plane, as well as the memory to recall all the different echoes, strong and weak. This image becomes recognizable, particularly with practice. The recognizable image can then be evaluated for abnormalities, and measured.

B-mode imaging was the first practical application of ultrasound for diagnostic purposed. The ability to appreciate the structures within a two-dimensional image is very much enhanced by visualizing the changes that occur within that image over time. A real-time image is still a 2-dimensional view, but one that is constantly updated. This then becomes 3-dimensional imaging (height, width, and time). Real-time sonography is most useful when the visualized object is moving (like a fetal heart), but is also valuable when the transducer beam is swept through the object, enhancing the operator's appreciation for details, texture, and shape.

Watershed segmentation is a way of automatically separating or cutting apart particles that touch. It starts with a mask or binary image, where the particles are for instance black. It calculates a distance map to find the fattest parts of the object (the peaks or local maxima of the distance map). Starting with the peaks as maximal erosion points (MEP's), it dilates them as far as possible - either until the edge of the object is reached, or the edge of the region of another growing MEP.

LabVIEW is ideally suited to any application that needs to combine conventional image analysis with other types of I/O. IMAQ Vision Toolkit is a complete set of functions for image processing. The IMAQ Vision Toolkit offers access to very sophisticated image processing tools from within the easy-to-use, consistent *look-and-feel* of LabVIEW. The morphology functions for the IMAQ Vision Builder's menus are: 1) Basic and Advanced Morphology in the Binary Menu and 2) Gray Morphology in the Grayscale menu.

2. Morphological Segmentation

In the analysis of the objects in images it is essential that we can distinguish between the objects of interest and the rest. This latter group is also referred to as the background. The techniques that are used to find the objects of interest are usually referred to as *segmentation techniques* - segmenting the foreground from background. In some image analysis and machine vision applications — such as industrial defect inspection or biomedical imaging — segmentation based on thresholding or edge detection is not sufficient because the image quality is insufficient or the objects under inspection touch or overlap. In such applications, morphological segmentation is an effective method of image segmentation.

Morphological segmentation partitions an image based on the topographic surface of the image. The image is separated into non-overlapping regions with each region containing a unique particle. Thresholding can segment objects from the background only if the objects are well separated from each other and have intensity values that differ significantly from the background. Binary morphology operators, such as close or open, often return inaccurate results when segmenting overlapping particles.

It is necessary to use morphological segmentation to segment touching or overlapping objects from each other and from the background. Also, use morphological segmentation when the objects have intensity values similar to the background.

Morphological segmentation is a multiple-step process involving several NI Vision functions. The following list describes each morphological segmentation step.

1. The use of a global or local threshold to create a binary image.

2. If necessary, use binary morphology operations to improve the quality of the image by filling holes in particles or remove extraneous noise from the image.

3. Use the Danielsson function to transform the binary image into a grayscale distance map in which each particle pixel is assigned a gray-level value equal to its shortest Euclidean distance from the particle border.

4. Perform a watershed transform on the distance map to find the watershed separation lines.

5. Superimpose the watershed lines on the original image using an image mask.

Fig.1 summarizes the morphological segmentation process and shows an example of each step.
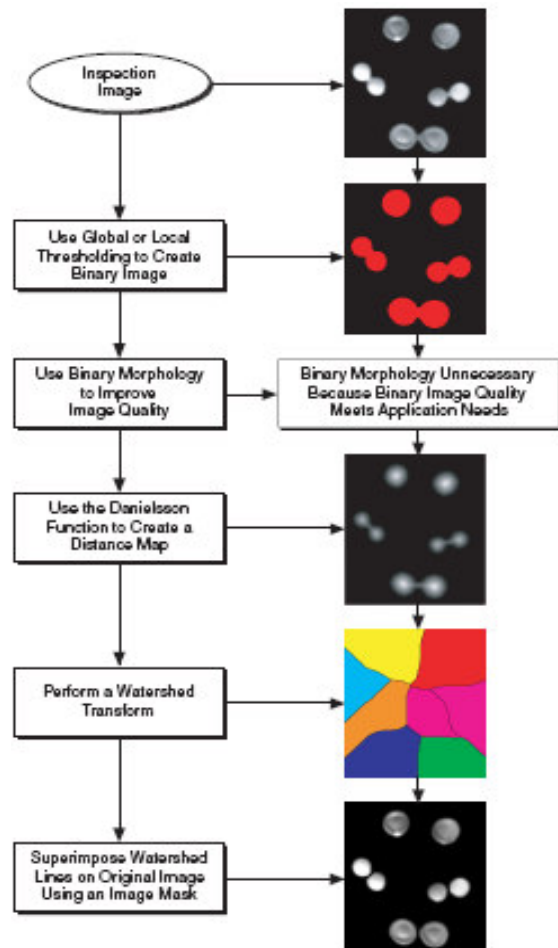

Fig.1. Morphological segmentation process.

In geography, a watershed is an area of land from which all rain that falls on the land flows into a specific body of water. In imaging, the watershed transform algorithm considers the objects under inspection to be the bodies of water. Figure 2 illustrates this concept.

Figure 2a shows an inspection image after it has been thresholded. Figure 2b shows the distance map of objects in the image using the gradient palette. Figure 2c shows the topographic surface of the distance map. Each object from the inspection image forms a deep, conical lake called a catchment basin. The pixels to which the distance map function assigned the highest value represent the deepest parts of each catchment basin. The image background represents the land surrounding the catchment basins. To understand how a watershed transform works, imagine that the catchment basins

are dry. If rain were to fall evenly across the image, the basins would fill up at the same rate. Eventually, the water in the basins represented by the circle and square would merge, forming one lake. To prevent the two lakes from becoming one, the watershed transform algorithm builds a dam, or *watershed line*, where the waters would begin to mix.
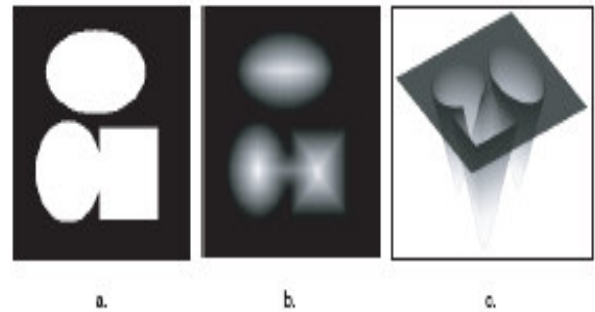

Fig.2. 3D View of a Distance Map.

Fig. 3a shows the same distance map as Fig. 2b with a line through the bottom two objects. Fig. 3b shows the intensities of the pixels along the line in Fig.3a. Notice the watershed line preventing the waters from the two catchment basins from mixing.
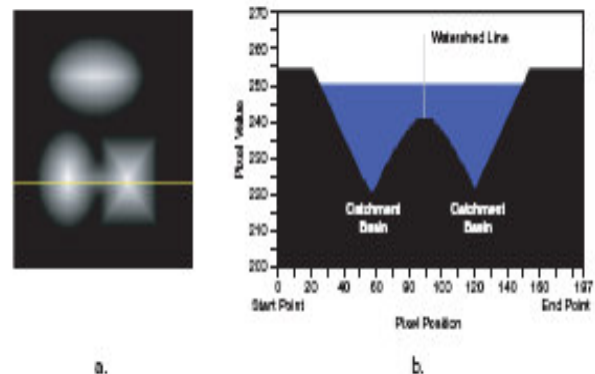

Fig.3. Watershed line.

As the rainfall continues, the rising water in all three lakes would begin to flood the land. The watershed transform algorithm builds dams on the land to prevent the flood waters from each lake from merging. Fig. 4 shows the watershed transform image after segmentation is complete. The water from each catchment basin is represented by a different pixel value. The black lines represent the watershed lines.

Echocardiography (ultrasound imaging of the heart) has been one of the driving application areas of medical ultrasound and the literature on methods for automatically segmenting and tracking the left ventricle (the normal chamber assessed for heart disease) is extensive.
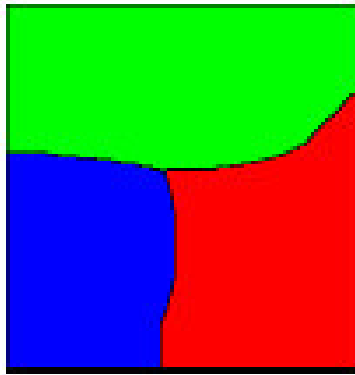
Fig.4.Inspection Image Segmented with Watershed
Lines.

Most attention has been given to tracking the motion of the endocardium (blood pool/tissue border) to allow for estimation of left ventricular areas/volumes and a derived measure, such as the ejection fraction, for regional wall motion assessment. In particular, these measures are used in diagnosis and assessment of ischaemic heart disease. Most analysis is based on 2-D acquisitions in which it is implicitly assumed that the principal component of motion is in the plane of the acquisition slice. The standard 2-D diagnostic views used for this are called the parasternal short-axis (SAX), and apical four-chamber (4C), two-chamber (2C), and three-chamber (3C) views. The latter three are also sometimes referred to as (apical) long-axis (LAX) views. The quality of data, and hence challenges for segmentation, vary depending on the view due to the anisotropy of ultrasound image acquisition, artefacts such as shadowing from the lungs, and attenuation which can be strong. Segmentation methods should also have strategies for avoiding the papillary muscles. Reliably finding the outer wall (often called epicardial border detection) is much more challenging, particularly from apical views. There are many papers on left ventricle tracking which deal with the tracking/deformation model independent of feature extraction or the imaging modality.

3 Watershed transform

The watershed transform is a powerful building block for morphological partitioning. In particular, a very powerful gray-scale segmentation methodology results from applying the watershed to the morphological gradient of an image to be segmented.

We shall focus only on the basic approach and leave more recent developments to the literature.

Let it be said that the watershed methodology has been highly developed so as to deal with numerous real-world contingencies, and various implementation algorithms have been developed.

The watershed transform is the method of choice for image segmentation in the field of mathematical morphology.

In grey scale mathematical morphology the watershed transform, originally proposed by Digabel and Lantuéjoul [5] and later improved by Beucher [6], is the method of choice for image segmentation.

Generally spoken, image segmentation is the process of isolating objects in the image from the background, i.e., partitioning the image into disjoint regions, such that each region is homogeneous with respect to some property, such as grey value or texture.

The watershed transform can be classified as a region-based segmentation approach. The intuitive idea underlying this method comes from geography: it is that of a landscape or topographic relief which is hooded by water, watersheds being the divide lines of the domains of attraction of rain falling over the region.

A watershed definition for the continuous case can be based on distance functions. Depending on the distance function used one may arrive at different definitions. Assume that the image f is an element of the space $C(D)$ of real twice continuously differentiable functions on a connected domain D with only isolated critical points.

Then the topographical distance between points p and q in D is defined by

$$T_f(p,q)=\inf_\gamma \int_\gamma \|\nabla f(\gamma(s))\| ds \qquad (1)$$

where the infimum is over all paths (smooth curves) inside D with $\gamma(0)=p$, $\gamma(1)=q$.

The topographical distance between a point $p\in D$ and a set $A\subseteq D$ is defined as $T_f(p,A)=MIN_{a\in A}T_f(p,a)$.. The path with shortest T_f -distance between p and q is a path of steepest slope.

This motivates the following rigorous definition of the watershed transform:

Let $f\in C(D)$ have minima $\{m_k\}_{k\in I}$, for some index set I.

The catchment basin $CB(m_i)$ of a minimum m_i is defined as the set of points $x\in D$ which are topographically closer to m_i than to any other regional minimum m_j like in equation (1):

$$CB(m_i) = \left\{ x \in D \middle| \forall j \in I \setminus \{i\} : f(m_i) + T_f(x, m_i) < f(m_j) + T_f(x, m_j) \right\}$$

The watershed of f is the set of points, which do not belong to any catchment basin:

$$Wshed(f) = D \cap \left(\bigcup_{i \in I} CB(m_i) \right)^c \qquad (2)$$

Let W be some label, $W \notin I$. The watershed transform of f assigns labels to the points of D, such that first different catchment basins are uniquely labeled, and second a special label W is assigned to all points of the watershed of f.

It is possible to extend the definition for three dimensional real-time images, taking into account that $x \in D$ and $y \in E$ are topographically closer to m_i than to any other regional minimum m_j, in following way:

$$CB(m_i) = \{ x \in D, y \in E \middle| \forall j \in I \setminus \{i\} : f(m_i) + \\ + T_f(x, y, m_i) < f(m_j) + T_f(x, y, m_j) \} \qquad (3)$$

The new watershed of f will contain the new $CB(m_i)$.

A classical approach to the production of edge images is to apply a gradient and then threshold the resulting gradient image to produce a binary edge image. There are many difficulties in this approach. One is the selection of an appropriate threshold value. Even if we ignore the problem of producing false edges by choosing too low a threshold, problems remain. If the threshold is too low, then the edges are very wide and must undergo severe thinning, which might leave them inaccurate; if the threshold is too high, then many edges will not be detected and those that are may be severely broken.

There are many watershed algorithms in the literature. One of the best and intuitive definitions of the watershed transform is the one based on the flooding simulation. Consider the input gray-scale image as a topographic surface. The problem is to produce the divide-line image on this surface. To do so, holes are punched in the marker regions. Each marker is associated to a color. The topography is flooded from below by letting colored water rise from the holes with its associated color, at a uniform rate across the entire image. When the rising water of distinct colors would merge, a dam is built to prevent the merging. The flooding will eventually reach a stage when only the tops of dams are visible above the waterline, and these correspond to the divide lines WS of the watersheds.

The colored regions are the catchment basins CB associated to each marker. In the classical watershed transform, the surface is punched on all regional minima and the watershed splits the image in primitive catchment basins.

The power of the watershed transform is revealed when we can creatively design the input function and the marker. There are mainly three categories of input image: gradient, negate of the distance transform, and the input image as it is. Next, we will explore the applications of the watershed when computed on the negation of the distance transform. The Voronoi diagram [7] is a partition of space into regions, each of which consists of the points closer to one particular object than to any others. In morphology, the term influence zone is often used as a synonim of the Voronoi diagram. The SKeleton by Influence Zones (or SKIZ) is composed of the boundaries of the various influence zones. The watershed transform is a suitable method to compute the Voronoi diagram and the SKIZ. The idea is to compute the classical watershed transform of the distance transform of the background of the objects. The catchment basins are the Voronoi diagram and the watershed lines are the SKIZ. Voronoi diagrams have a surprising variety of uses:

a) *Nearest neighbor search* -- For a query point q, finding its nearest neighbor from a fixed set of points S is simply a matter of determining which cell in the Voronoi diagram of S contains q.
b) *Facility location* -- This location is always at a vertex of the Voronoi diagram, and it can be found in a linear-time search through all the Voronoi vertices.
c) *Largest empty circle* -- A Voronoi vertex defines the center of the largest empty circle among the points.
d) *Path planning* -- If the sites of S are the centers of obstacles we seek to avoid, the edges of the Voronoi diagram define the possible channels that maximize the distance to the obstacles.

Thus in planning paths among the sites, it will be *safest* to stick to the edges of the Voronoi diagram. We address the problem of binary-image segmentation from the perspective of there being objects within the image that are touching or overlapping. This was one of the earliest application of the watershed. Our goal is to segment the single component in a manner consistent with the integrity of each of the two objects.

A key to this problem, and to many segmentation problems, is to find markers for each of the two objects.

4. Real Time 3D Image Processing Methodology

Texture features and gray-level intensity are useful for myocardial classification. In our method, segmentation is conducted in a multifeature vector space. Four texture features are employed together with the gray-level intensity to construct the multifeature vector space.

Ten texture analysis methods are employed to compute the digital ICE video images. Among them, five are conventional methods including the *gray value run length* (GVRL), the *gray value cooccurrence matrix* (GVCOM), the *gray value and gradient co-occurrence matrix* (GGCOM), the local power spectrum, and the adaptive filtering. The size of the local window is 9x9 pixels. The other two methods developed here use the wavelet transform to analyze the texture properties in multiple scales. The first method calculates the sum of the local *wavelet energy signature* in three scales and all three directions. The second method introduces six wavelet detail histogram signatures, which captures all first order statistics using a model-based approach. For these two wavelet methods, a 32x32 local pixel window is used. In the last three methods, images are decomposed into three scales with two-dimensional wavelet transform. Only the detail parts of each scale are reconstructed back to the spatial domain while smooth parts at the same scale and details and smooth parts in other scales are set to zero. Three reconstructed images are obtained. Each of them contains information within one scale. Then, GVCOM, GVRL, and GGCOM methods are used to obtain second-order texture properties from the reconstructed images (9x9x9 voxels volumetric subimage).

The four selected texture features are as follows:
1) The local gray-level variance (VAR) as in equation (4):

$$\sigma^2(x_v, y_v, z_v) =$$

$$= \frac{1}{w^2} \sum_{m=-w/2}^{w/2} \sum_{n=-w/2}^{w/2} \sum_{l=-w/2}^{w/2} \left(f_{x_v-m, y_v-n, z_v-l} - mean_{w \times w \times w} \left(f_{x_v, y_v, z_v} \right) \right) \quad (4)$$

where f_{x_v, y_v, z_v} is the gray-level intensity at voxel v, $wxwxw$ is the size of the local three-dimensional structure.

2) The high gray-level run emphasis (HGRE) from the gray run length analysis :

$$HGRE(x_v, y_v, z_v) = \sum_{i=1}^{M} \sum_{j=1}^{N} \sum_{l=1}^{K} R(i, j, l) / s \quad (5)$$

where $R(i, j, l)$ is a volumetric element of the local run length matrix at voxel v, s is the total number of runs in the volumetric subimage. M is the number of gray levels, N is the longest run and K is the number of longitudinal image slices.

3) The sum of the local wavelet energy signatures (SLWES):

$$SLWES(x_v, y_v, z_v) = \sum_{n,i,p} \left(\frac{1}{N} \sum_{j,k} \left(D_{nip}(j, k) \right)^2 \right) \quad (6)$$

$$n = 1,2,3, \quad i = 1,2,3, \quad p = 1,2,3.$$

where n is the scale and i, p is one of the three different directions of the detail volumetric image. $D_{nip}(j, k)$ are the details in scale n and direction i and p. N is the number of voxels in each detail image.

4) The inertia of the gray value co-occurrence matrix:

$$Inertia(x_v, y_v, z_v) = \sum_{i=1}^{N_g} (i - j - k)^2 G(i, j, k) \quad (7)$$

where N_g is the maximal gray value. $G(i, j, k)$ are the amount of the voxels, which are specific for a gray value in a volumetric subimage.

If we take slices of the whole presented three dimensional image it is possible to observe that the free voxel v will be merged into class K if the following conditions is satisfied.

$$\left\| \vec{V}(x_v, y_v, z_v) - \vec{V_K} \right\| \le Median \left(\left\| \vec{V}(x_v, y_v, z_v) - \vec{V_i} \right\| \right) \quad (8)$$

$$(i = 1........C).$$

$\vec{V_i}$ is the characteristic vector of class i. C is the number of classes. When there are two or more classes that have *geographic priority privilege* GPP to voxel v, the one with a minimum Euclidean distance to voxel v will capture voxel v if that distance is less than or equal to the median value of the distances between voxel v and all of the classes. Using this criterion, the image can be segmented successfully.

Equal opportunity competence EOC criterion is used to make results independent of processing order. Only voxels at the edge of the seed regions at

the beginning of a growing circulation are permitted to grow during the growing circulation.

In our region growing method, processing order is potentially problematic because the *geographic similarity* GS criterion allows merging of a pixel into a class despite the pixel not having the shortest feature distance to that class (provided the region of this class is geographically close to the pixel). These results in a possibility that a voxel can be merged into different classes and the class who reaches the voxel first will get the voxel. If, during the region growing circulation, a recently classified voxel is allowed to classify its neighboring free voxels, then the class region that is processed first will grow faster and will have a greater chance to be geographically closer to a free voxel.

The segmentation procedure for 3D echographic images is shown in Fig.6., in addition the procedure is implemented in LabVIEW.
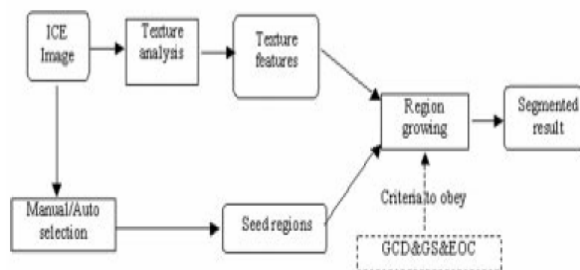
Fig.6. Segmentation procedure for three dimensional biomedical images.

The fundamental criteria to obey are: GCD-global comparison detection, GS-geographic similarity, EOC-equal opportunity competence.

Step 1) *Texture Analysis:* The four features are calculated in the region of interest ROI. The multifeature space is constructed using these four features and the gray-level intensity.

Step 2) *Seed Region Selection:* For a more robust estimation of the class characteristic vector, we select rectangular seed regions rather than seed points. The rectangular seed region for one class should be inside of the whole class region but not necessarily in the center. These initial seed regions are termed $Seed_i, i = 1,2,...,C$, where C is the number of classes. The seed regions were manually selected by a specialist according to the gross pathology images [8], [9]. We also tested our method using seed region selection guided only by visual evaluation of ICE images of the myocardium after reperfusion.

Step 3) *Calculation of Characteristic Vectors:* The initial characteristic vector of each class is calculated as the average of the

characteristic vector of each pixel inside the class's seed region, e.g., the characteristic vector of class C, $\vec{V}_k$ is

$$\vec{V}_k = \frac{1}{m \times n \times l} \sum_{v \in Seed_k} \vec{V}(x_v, y_v, z_v) \qquad (9)$$

where $m \times n \times l$ is the size of the seed region.

Step 4) *Region Growing:* The region growing procedure starts from the seed regions. The first border voxel BV is termed BV_1. Then based on the GCD, EOC and GS criteria, region growing is carried out and the BV set is updated, after each region growing circulation. After the n-th growing circulation, the characteristic vector of class C is updated. $Number_C^n$ is the number of voxels in class C at the start of the current n*th* growing circulation. N_c^n is the number of voxels captured in the *n*th growing circulation. T is the set of just classified voxels during *n*th growing circulation. $Feature_{j(n(C))}$ is the *j*th feature value for voxel $n(C)$ in T. The growing circulation repeats until no more voxels can be classified.

Cardiologists also use a movie of a heart in decision-making as the speckle pattern associated with deforming tissue can be observed in a movie whereas in a still frame the speckle pattern is not always useful. As a result, and in contrast to some other clinical application areas, in echocardiography it is perhaps more logical to view segmentation as a spatio-temporal problem. More recent successful approaches have taken this viewpoint.

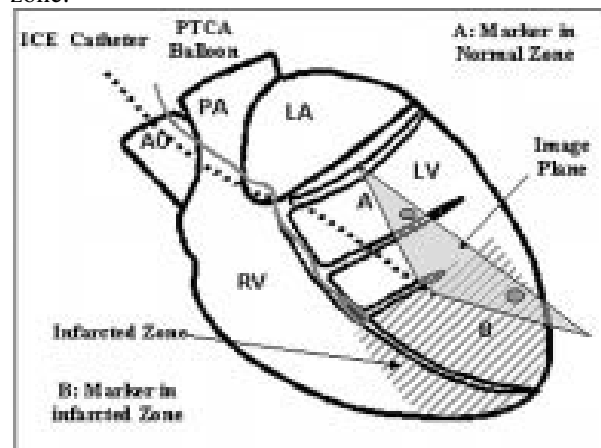In Fig.7. is presented the marker in the normal zone of the heart and the marker in the infarcted zone.

Fig.7. Schematic representation of bead location on the epicardial surface in relation to the abnormal region and positioning of the intracardiac ultrasound catheter. The ultrasound catheter was placed in the left ventricle via the carotid artery.
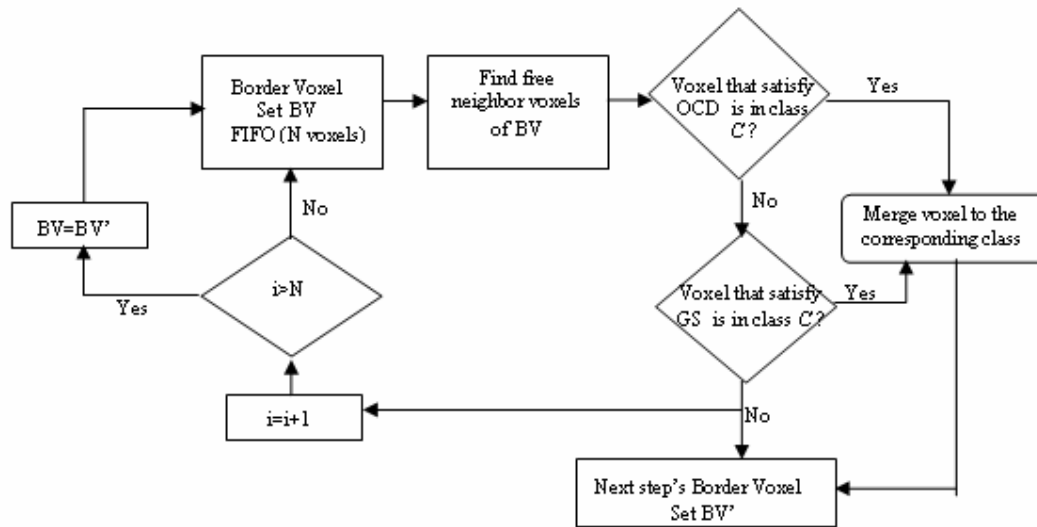
Fig.8. Flowchart of region growing circulation.

Fig.8. shows the details of region growing controlled by criteria mentioned above.

The following steps illustrate the LabVIEW and Vision implemented method *VoxelSeg* of segmenting objects.

 1.*Threshold*—(**Grayscale»Threshold**) *Threshold* the image to isolate the objects we want to segment from the rest of the image.

2.*Remove   Noise*—(**Binary»Advanced Morphology** or **Binary»Particle Filter**) Remove extraneous information from the binary image using various morphology operations. For example, we can fill in holes with the Advanced Morphology option *Fill holes* or remove noise with the *Particle Filter* function.

3.*Create   Distance   Map*—(**Binary»Advanced Morphology**) Use the *Danielsson* option to transform the binary image into a grayscale image in which the center of each object represents a local maximum in the image. If you were to look at the topographical surface of the image after applying the distance map, each object would appear as a smooth, gradual peak.

4.Apply   *Watershed   Transform   —* (**Grayscale»Watershed Segmentation**) Apply the watershed transform to segment the image into

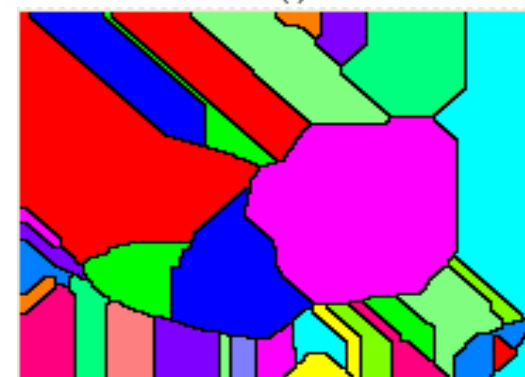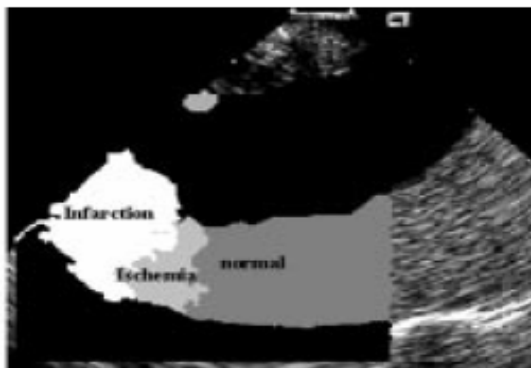local zones. A zone is determined by the watershed line that separates the influence zone of each peak.

(a)

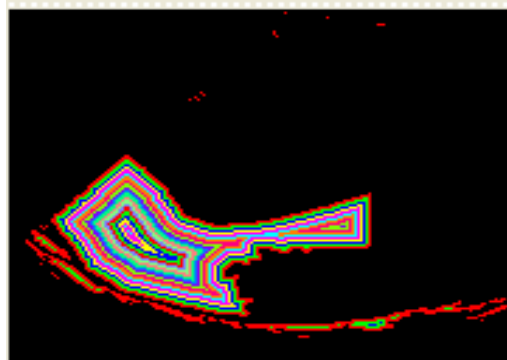Fig.9. a) Watershed segmented echocardiography without EOC criterion.

(b)

Fig.12. Distance map (Danielsson) on echocardiography without EOC criterion.

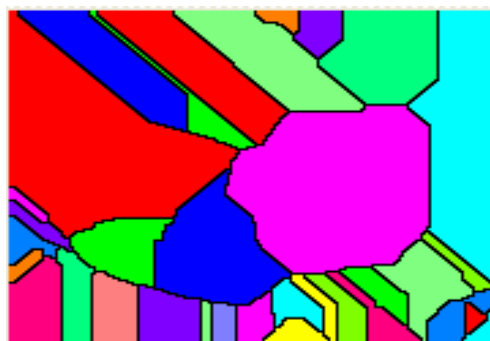Fig.9. b) Watershed segmented echocardiography with EOC criterion.

Fig.13. Watershed segmentation on echocardiography without EOC criterion.

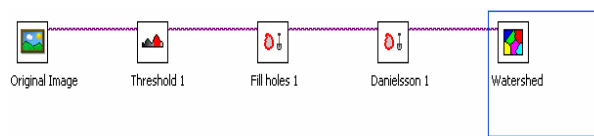The implemented LabVIEW and Vision script is the following:

Fig.14. Implemented LabVIEW and Vision script for real-time 3D echocardiography processing.

Fig.10. Threshold on echocardiography without EOC criterion.

Fig.11. Fill holes on echocardiography without EOC criterion.

Fig.15. Threshold on echocardiography with EOC criterion.

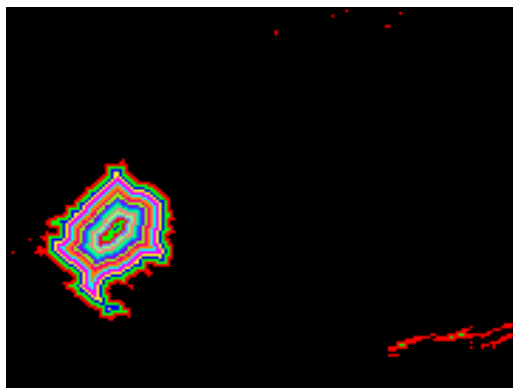Fig.16. Fill holes on echocardiography with EOC criterion.

Fig.17. Distance map (Danielsson) on echocardiography with EOC criterion.
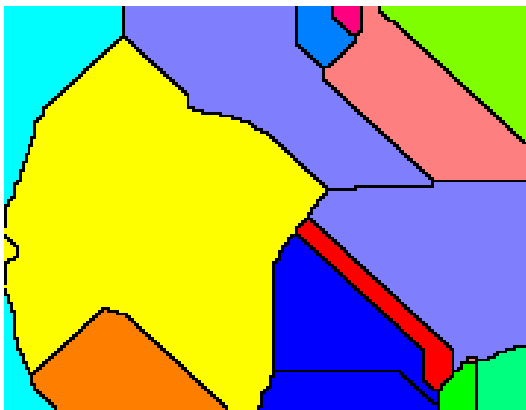

Fig.18. Watershed segmentation on echocardiography with EOC criterion.

The yellow field indicates a great problem concerning an infarction.

Finally, there is a very limited literature explicitly looking at segmentation and analysis of the myocardium and epicardial border detection. These are both challenging to do from native - mode images. There is also very little literature specifically focussed on getting methods to work on general clinical data rather than data from subjects with a good acoustic window i.e., which give good images.
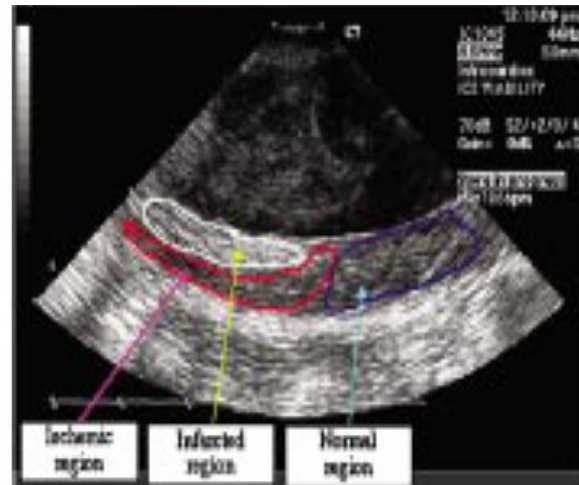

Fig.17. Three regions indicated by a cardiologist according to the pathology image.

We have highlighted some segmentation methods that have been done above. One further exception is the work of Boukerroui *et al.* [1] which considers how to enhance – mode images to reduce the affect of attenuation and enhance features. Although that method was shown quantitatively to reduce attenuation, enhance features, and not introduce artefacts after enhancement, that approach has not to-date been fully tested in clinical practice.

Comparing the watershed segmentation on echocardiography with EOC criterion with the image indicated by the cardiologist it is possible to recognize that the yellow field indicates a great problem concerning an infarction.

5 Conclusion

In the past, dynamic cardiac 3D rendered images were possible by sequentially acquiring 2D images and then using a workstation to input 2D images for Cartesian coordinate conversion and volume rendering. Outside research settings, this time-consuming process proved cumbersome and was simply impractical.

Now that these technical and practical issues have been addressed, realtime 3D cardiac sonography has great potential to impact both patient care and throughput in a number of ways, including better pre- and post-surgical planning, improved measurement of heart function, decreased exam times, and enhanced communication between clinicians and their patients. With real-time 3D

cardiac ultrasound images, clinicians will be able to better quantify size, shape and function of the heart. However, the most important contribution of real-time 3D sonography in cardiology may be improvement in locating abnormalities for surgical planning.

The new technology will also provide important information regarding surgical outcomes. A great benefit to obtaining more diagnostic information and higher diagnostic confidence from real-time 3D cardiac ultrasound images is that it could lead to more rapid exam times and the reduction of patient wait times. Being able to see the whole heart makes examinations more simple and rapid, benefiting the staff and patient. The utility of this technology is unusually broad, as it is able to move beyond diagnostics into a key role in therapeutic procedures. As with any new technology, there will be a learning curve to understanding 3D imaging. Though the matrix transducer is somewhat larger than a standard 2D probe, the ergonomics are quite similar. The interface of the ultrasound unit is in generally very user friendly.

Because real-time 3D cardiac ultrasound involves looking at the heart as if you are holding it in your hands, with the additional ability to turn it any way you want, we expect that the transition from 2D to 3D will be easily achieved and implemented.

We tested the method in images with seed regions placed in accordance to the pathology images. Ten images with infarcted myocardium were selected from diastolic frames in which both epicardial bead markers could be clearly seen. These images were acquired at the end of the ischemic period and during reperfusion. Our goal was to segment ischemic viable, ischemic nonviable (infarcted), and normal myocardium. Myocardium was outlined by a specialist to simplify segmentation. Seed regions were manually selected by a cardiologist according to the gross pathology images. Myocardium in each ICE image was segmented using our new method.

The EOC (equal opportunity competence) criterion is very important in highlighting the infarcted zone. The shape and spatial distribution of segmented infarction and ischemic regions are close to the corresponding regions in the gross pathology images.

It took approximately 40s for region growing with software programming in C++ language and approximately 10s for region growing with software programming in LabVIEW.

References:

[1] J. A. Noble and D. Boukerroui, Ultrasound image segmentation: A survey, *IEEE Trans. Med. Imag.*, vol. 25, no. 8, pp. 987–1010, Aug.2006.

[2] O.T. von Ramm, S.W. Smith, Real time volumetric ultrasound imaging system, *J.Digit.Imag*, vol.3, no.4, pp.261-266, Nov.1990.

[3] T.Binder,Three - dimensional echocardio-graphy - Principles and promises, *J. Clin. Basic Cardiol.,* vol. 5, no.2, pp.149-152, 2002.

[4] M. Franke, H.P. Kohl, Second-generation real-time 3-D echocardiography: A revolutionary new technology, Medicamundi, vol.47, no.2, p.3440, 2003.

[5] H. Digabel, C.Lantuéjoul, Iterative algorithms, in Proc. 2nd European Symp. Quantitative Analysis of Microstructures in Material Science, Biology and Medicine, Caen, France, pp.85-99, 1978.

[6] S. Beucher, Algorithmes sans biais de ligne de partage des eaux, *CMM Internal note,* Paris, School of Mines, 2004.

[7] W. L. Roque, D. Doering, Constructing Approximate Voronoi Diagrams from Digital Images of Generalized Polygons and Circular Objects, *WSG*, Feb.3-7, Plzen Czech Republic, 2003.

[8] X. Hao, C.J. Bruce, C Pislaru, J. Greenleaf, Segmenting High-Frequency Intracardiac Ultrasound Images of Myocardium into Infarcted, Ischemic and Normal Regions, *IEEE Transactions on Medical Imaging,* vol.20, no. 12, pp. 1373-1383, 2001.

[9] J. G. Bosch, S. C. Mitchell, B. P. F. Lelieveldt, F. Nijland, O. Kamp, M. Sonka, and J. H. C. Reiber, Automatic segmentation of echocardiographic sequences by active appearance motion models, *IEEE Trans. Med. Imag.*, vol. 21, no. 11, pp. 1374–1383, Nov. 2002.